




Excessive tubulin polyglutamylation causes neurodegeneration and perturbs neuronal transport

Maria M Magiera^{1,2,*} , Satish Bodakuntla^{1,2} , Jakub Žiak^{3,4}, Sabrina Lacomme⁵, Patricia Marques Sousa^{1,2,†}, Sophie Leboucher^{1,2}, Torben J Hausrat⁶, Christophe Bosc^{7,8}, Annie Andrieux^{7,8}, Matthias Kneussel⁶, Marc Landry⁹, André Calas⁹, Martin Balastik³ & Carsten Janke^{1,2,**} 

Abstract

Posttranslational modifications of tubulin are emerging regulators of microtubule functions. We have shown earlier that upregulated polyglutamylation is linked to rapid degeneration of Purkinje cells in mice with a mutation in the deglutamylating enzyme CCP1. How polyglutamylation leads to degeneration, whether it affects multiple neuron types, or which physiological processes it regulates in healthy neurons has remained unknown. Here, we demonstrate that excessive polyglutamylation induces neurodegeneration in a cell-autonomous manner and can occur in many parts of the central nervous system. Degeneration of selected neurons in CCP1-deficient mice can be fully rescued by simultaneous knockout of the counteracting polyglutamylase TLL1. Excessive polyglutamylation reduces the efficiency of neuronal transport in cultured hippocampal neurons, suggesting that impaired cargo transport plays an important role in the observed degenerative phenotypes. We thus establish polyglutamylation as a cell-autonomous mechanism for neurodegeneration that might be therapeutically accessible through manipulation of the enzymes that control this posttranslational modification.

Keywords axonal transport; neurodegeneration; tubulin code; tubulin polyglutamylation; tubulin posttranslational modifications

Subject Categories Cell Adhesion, Polarity & Cytoskeleton; Neuroscience; Post-translational Modifications, Proteolysis & Proteomics

DOI 10.15252/embj.2018100440 | Received 7 August 2018 | Revised 14 September 2018 | Accepted 20 September 2018 | Published online 12 November 2018

The EMBO Journal (2018) 37: e100440

See also: **V Shashi *et al*** (December 2018) and **A Akhmanova & CC Hoogenraad** (December 2018)

Introduction

The microtubule cytoskeleton is a key structural component of neurons, where it carries out a multitude of specialized functions. Microtubules are essential for establishing and maintaining neuronal polarity (Craig & Banker, 1994), regulating neuronal morphology (Liu & Dwyer, 2014), transporting cargo (Franker & Hoogenraad, 2013), and scaffolding signaling molecules to form signaling hubs (Dent & Baas, 2014). Consequently, dysfunction of microtubules can lead to neurodevelopmental disorders as well as to neurodegeneration. The role of the microtubule cytoskeleton in neuronal dysfunction has been widely recognized; however, it was usually associated with abnormalities in a variety of microtubule-interacting proteins (Millecamps & Julien, 2013; Brady & Morfini, 2017), the most prominent being the aggregation of the microtubule-associated protein tau in Alzheimer's disease (Wang & Mandelkow, 2016). More recently, the discovery of patients with mutations in genes encoding the building blocks of microtubules—the α - and β -tubulins—revealed that alterations of the microtubules themselves could be causative for a range of neurodevelopmental and neurodegenerative disorders (Chakraborti *et al*, 2016), most likely by subtly but significantly altering microtubule properties (Belvindrah *et al*, 2017). It is thus conceivable that, in a more general manner, mechanisms involved in fine-tuning intrinsic microtubule properties and functions could play causative roles in neuronal dysfunctions.

One such candidate mechanism is dysregulation of tubulin post-translational modifications (PTMs) that are expected to control many microtubule functions in cells, by either changing the physical properties of microtubules or by regulating their interactions with other cellular components (Janke, 2014). MTs can carry a large number of PTMs, such as acetylation, polyglutamylation,

1 Institut Curie, CNRS UMR3348, PSL Research University, Orsay, France

2 Université Paris-Saclay, CNRS UMR3348, Université Paris Sud, Orsay, France

3 Department of Molecular Neurobiology, Institute of Physiology, Czech Academy of Sciences, Prague 4, Czech Republic

4 Faculty of Science, Charles University, Prague 2, Czech Republic

5 Bordeaux Imaging Center, BIC, UMS 3420, Université Bordeaux, Bordeaux, France

6 Center for Molecular Neurobiology (ZMNH), University Medical Center Hamburg-Eppendorf, Hamburg, Germany

7 Grenoble Institut des Neurosciences, GIN, Université Grenoble Alpes, Grenoble, France

8 Inserm U1216, Grenoble, France

9 Interdisciplinary Institute for Neuroscience, CNRS UMR5297, Université Bordeaux, Bordeaux, France

*Corresponding author. Tel: +33 1 69863127; Fax: +33 1 69863017; E-mail: maria.magiera@curie.fr

**Corresponding author. Tel: +33 1 69863127; Fax: +33 1 69863017; E-mail: carsten.janke@curie.fr

†Present address: Harvard Medical School, Children's Hospital Boston, Boston, MA, USA

polyglycylation, and detyrosination. Polyglutamylation, a PTM that is particularly enriched on neuronal microtubules (Janke & Bulinski, 2011), adds variable numbers of glutamate residues as secondary branches to the main tubulin chain (Eddé *et al*, 1990), thus generating a range of graded signals. This predestines polyglutamylation to be a fine-tuning mechanism of microtubule functions, a principle that has recently been proven for the best-studied function of this PTM, the control of spastin-mediated microtubule severing (Lacroix *et al*, 2010; Valenstein & Roll-Mecak, 2016). Polyglutamylation is further expected to regulate intracellular trafficking; however, so far only initial insights into the role of this PTM in molecular-motor tuning are available (Sirajuddin *et al*, 2014).

The recent discovery of a large number of tubulin-modifying enzymes now allows to directly address the role of tubulin PTMs (Janke, 2014). Cytosolic carboxypeptidases (CCPs) (Kalinina *et al*, 2007; Rodriguez de la Vega *et al*, 2007) are a class of tubulin-modifying enzymes that remove acidic amino acid residues from the carboxy-termini of peptide chains (Rogowski *et al*, 2010; Berezniuk *et al*, 2012), thus controlling two major types of PTMs: First, they reverse polyglutamylation, a PTM catalyzed by polyglutamylases from the tubulin-tyrosine ligase-like (TTL) family (Janke *et al*, 2005; van Dijk *et al*, 2007), and second, CCPs can remove C-terminal, gene-encoded glutamate residues, which converts α -tubulin into $\Delta 2$ - and $\Delta 3$ -tubulins (Rogowski *et al*, 2010; Aillaud *et al*, 2016) or affects other proteins with acidic C-termini (Tanco *et al*, 2015). Impaired deglutamylase activity was initially linked to neurodegeneration in a mouse model with early loss of the Purkinje cells in the cerebellum, the *Purkinje cell degeneration (pcd)* mouse (Mullen *et al*, 1976). This mouse carries a mutation in the *CCP1* gene (Fernandez-Gonzalez *et al*, 2002), which causes accumulation of polyglutamylation in the cerebellum (Rogowski *et al*, 2010). However, whether deregulation of this PTM directly causes the degeneration of the Purkinje cells, whether impaired deglutamylase activity is universally deleterious to neurons, and which are the underlying molecular mechanisms have remained open questions. In the present study, we establish excessive polyglutamylation as a general, cell-autonomous cause of neurodegeneration that induces transport defects in neurons. We further show that by manipulating enzymes catalyzing polyglutamylation, it is possible to protect neurons against hyperglutamylation-induced neurodegeneration.

Results

Excess of TTL1-mediated polyglutamylation causes neurodegeneration in a cell-autonomous manner

In *pcd* mice, mutation of the deglutamylase CCP1 leads to strongly upregulated levels of polyglutamylation in brain regions known to degenerate, such as the cerebellum or the olfactory bulb (Mullen *et al*, 1976; Rogowski *et al*, 2010). While this suggested that excessive polyglutamylation could be causative for neurodegeneration in these mice, it was unclear whether polyglutamylation damages neurons in a cell-autonomous as opposed to a tissue-wide manner.

To answer this question, we generated *Ccp1^{flox/flox} L7-cre* mice. In the brain, the L7 promoter is only active in Purkinje cells (Rico

et al, 2004); therefore, *CCP1* is deleted specifically in these neurons. At 4 months of age, *Ccp1^{flox/flox} L7-cre* mice showed ataxia comparable to *Ccp1^{-/-}* or *pcd* mice, and had lost most, though not all of the Purkinje cells (see Fig 1A and F). The partial survival of the Purkinje cells at 4 months is most likely due to the late activation of the L7 promoter in certain regions of the cerebellum (Rico *et al*, 2004), and indeed, at 18 months, all Purkinje cells have degenerated (see Fig 1A and F, Appendix Fig S1). This demonstrates that the loss of CCP1 is a cell-intrinsic cause of neurodegeneration.

We next asked whether accumulation of polyglutamylation, rather than the impairment of the second enzymatic activity of CCP1, the removal of gene-encoded C-terminal acidic amino acids from tubulins or other proteins (Rogowski *et al*, 2010; Tanco *et al*, 2015), is causative for the degeneration of neurons lacking CCP1. To specifically reduce polyglutamylation exclusively in the Purkinje cells of *pcd* mice, we deleted the major brain polyglutamylase, TTL1 (Janke *et al*, 2005), in these neurons by combining the *pcd* (*Ccp1^{-/-}*), *Ttll1^{flox/flox}*, and *L7-cre* (Rico *et al*, 2004) alleles (Fig 1B). While in *pcd* mice Purkinje cells degenerate mostly in the first month after birth (Mullen *et al*, 1976), *Ccp1^{-/-} Ttll1^{flox/flox} L7-cre* mice had an entirely preserved Purkinje cell layers even at older ages up to 18 months (see Fig 1C, D and F, Appendix Fig S1). The absence of Purkinje cell degeneration throughout the entire lifespan of these mice demonstrates that excessive polyglutamylation catalyzed by TTL1 is the unique cause of neurodegeneration in *pcd* (*Ccp1^{-/-}*) mice. The result also excludes the possibility that the removal of gene-encoded glutamate residues by CCP1 is implicated in the disease mechanism, as TTL1 cannot interfere with this type of modification. This is illustrated by the unaltered levels of $\Delta 2$ -tubulin in the cerebellum of *Ttll1^{-/-}* mice (Fig 1E). Finally, the deletion of *TTL1* exclusively in Purkinje cells (Fig 1F) demonstrates that this mechanism functions in a cell-autonomous manner, thus excluding a tissue-wide effect that might have protected these cells in *Ccp1^{-/-} Ttll1^{-/-}* mice (Berezniuk *et al*, 2012).

Having established TTL1-mediated polyglutamylation as the leading cause of neurodegeneration in mice lacking CCP1, we ultimately wanted to know whether this role is related to the polyglutamylation of tubulin, or whether other proteins can also be polyglutamylated by TTL1. We compared cerebellar extracts from *Ttll1^{-/-}* and wild-type mice by immunoblot with the polyE antibody, which recognizes extended polyglutamate chains irrespective of the protein they are attached to (Rogowski *et al*, 2010). At normal protein load, *Ttll1^{-/-}* brain extracts are void of polyE-positive proteins, while wild-type brains show a unique, strong protein band corresponding to α -tubulin (Fig 1E). Even when we overloaded the electrophoresis gel heavily with the extracts (up to 20x), we could not detect any additional protein band apart from α - and β -tubulin (Fig 1E). This shows that in cerebellum, tubulin is by far the most predominant substrate of TTL1, therefore implying that the absence of Purkinje cell degeneration in *Ccp1^{-/-} Ttll1^{flox/flox} L7-cre* mice is directly caused by the reduction of tubulin polyglutamylation in these neurons.

Taken together, our results demonstrate that the degeneration of Purkinje cells in the absence of the deglutamylase CCP1 is a cell-autonomous process, which is induced by excess of tubulin polyglutamylation catalyzed by TTL1 (Fig 1B and F).

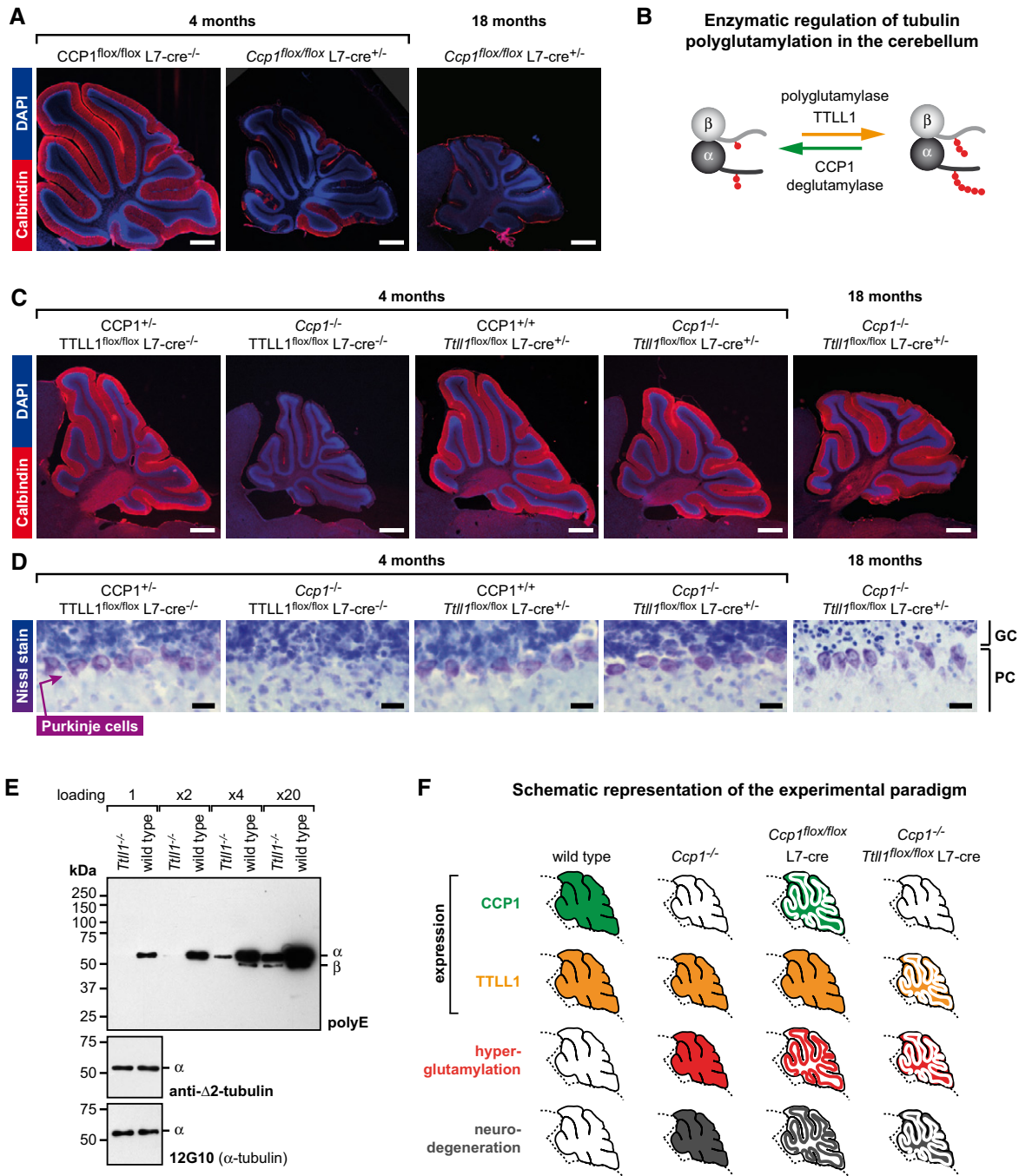


Figure 1. Excessive tubulin polyglutamylation induces Purkinje cell degeneration in a cell-autonomous manner.

- A Fate of Purkinje cells in mice with Purkinje-cell-specific knockout of *Ccp1*. *Ccp1*^{flox/flox} L7-cre mice show a massive but incomplete degeneration of Purkinje cells (calbindin-stained; red) at 4 months, while all Purkinje cells are degenerated at 18 months. Scale bar: 500 μm.
- B Schematic representation of enzymatic tubulin polyglutamylation (red points are glutamate residues that are posttranslationally added to C-terminal tails of α- and β-tubulin). In neurons, TTLL1 is generating a large share of the overall polyglutamylation (Janke et al, 2005), and CCP1 is reversing this PTM. Loss of CCP1 induces TTLL1-mediated hyperglutamylation, which can be avoided by TTLL1 inactivation.
- C Fate of Purkinje cells in mice with combinatorial knockout alleles. Knockout of *Ccp1* (*pcd* mouse; *Ccp1*^{-/-}) results in a complete degeneration of Purkinje cells (calbindin-stained; red), while the additional knockout of *Ttll1* selectively in the Purkinje cells (L7-cre) protects the entire Purkinje cell layer from degeneration up to 18 months. Scale bar: 500 μm.
- D Nissl staining of the Purkinje cell layer of the brains from various knockout mice shown in (C) confirms the absence of Purkinje cells in *Ccp1*^{-/-} and the presence of a wild-type-like Purkinje cell density in *Ccp1*^{-/-} *Ttll1*^{flox/flox} L7-cre mice. Scale bar: 20 μm. Purkinje cell layer (PC) and granule cell layer (GC) are indicated.
- E Immunoblot of tissue extracts from cerebella of *Ttll1*^{-/-} and wild-type mice, probed with the polyE, anti-Δ2-tubulin, and 12G10 antibodies. Increasing amounts of extracts were loaded for detection of polyglutamylated proteins with polyE.
- F Schematic representation of the experimental paradigm applied in this figure. The thick line in the cerebella symbolizes the Purkinje cell layer.

Excess of polyglutamylation can induce degeneration of different neuronal populations

In the *pcd* mouse, only some cell types and brain regions undergo degeneration, such as Purkinje cells in the cerebellum, mitral cells in the olfactory bulb (Mullen *et al*, 1976; Greer & Shepherd, 1982), thalamic neurons (O’Gorman & Sidman, 1985), and photoreceptors (LaVail *et al*, 1982; Bosch Grau *et al*, 2017). However, no obvious signs of neurodegeneration are seen in cerebral cortex and hippocampus, regions that are primarily affected in a range of late-onset human neurodegenerative disorders (Bretschneider *et al*, 2015). Based on findings in *pcd* mice, we had suggested that these regions are protected due to a strong expression of a second deglutamylase with similar specificity, CCP6 (Rogowski *et al*, 2010). This is supported by the observation that initially increased polyglutamylation levels in these regions return to normal in adult mice (Figs 2A and EV1). To test whether such a compensatory mechanism exists, we generated mice that effectively lacked both deglutamylases in the central nervous system using two different strategies (see Methods; referred to as *Ccp1^{-/-}Ccp6^{-/-}* hereafter). Elevated levels of tubulin polyglutamylation persisted in cerebral cortex and hippocampus of these mice, and even increased further upon aging (see Figs 2A and G, and EV1). As expected from the known enzymatic activities of CCP1 and CCP6, levels of $\Delta 2$ -tubulin were altered as well, mainly in young animals, while other tubulin PTMs were not, or only marginally, affected (Fig EV1).

To determine the impact of the *Ccp1^{-/-}Ccp6^{-/-}* double knockout on brain anatomy, we measured the thickness of motor and somatosensory cortices. While cortical thickness appeared normal at 1 month of age, it was significantly reduced at 5 months (Fig 2B and C, Appendix Fig S2), suggesting a degenerative process as opposed to a developmental defect. To confirm this, we quantified the number of pyramidal neurons (MAP2) and reactive astrocytes (GFAP) in cortical layer V as well as the density of apical dendrites of the pyramidal neurons (MAP2) in cortical layer IV (Figs 2D and EV2A and B, and EV3A and B). These analyses revealed a significantly decreased number of pyramidal neurons and their apical dendrites in the cortex of aging *Ccp1^{-/-}Ccp6^{-/-}* mice (Figs 2E and EV2C), which was

inversely correlated with a strong increase in reactive astrocytes (Figs 2E and EV3C). Decreased numbers of neurons and apical dendrites are hallmarks of cortical degeneration [e.g., in the premature aging mouse model, SAMP10 (Shimada *et al*, 2006), or in amyotrophic lateral sclerosis (Geevasinga *et al*, 2016)], and increase in reactive astrocytes is also consistent with neurodegeneration (Hol & Pekny, 2015). Finally, labeling with SMI-32 antibody (Kim *et al*, 2010) is strongly increased in the cerebral cortex of 2- and 5-month-old *Ccp1^{-/-}Ccp6^{-/-}* mice, but normal at 1 month (Fig 2F and Appendix Fig S3). Considering that SMI-32 is a marker of altered axonal transport and axonal damage (Watson *et al*, 1991), the progressive degeneration of the cerebral cortex could be linked to axonal defects. Moreover, as these defects coincide with persistent tubulin hyperglutamylation in *Ccp1^{-/-}Ccp6^{-/-}* cerebral cortices (Fig 2G), our observations suggest a more general role of hyperglutamylation in degeneration of neurons.

To determine the cellular basis of the observed degeneration in *Ccp1^{-/-}Ccp6^{-/-}* cerebral cortices, we performed ultrastructural analyses by transmission electron microscopy. Focusing on myelinated axons, we found that several axons of *Ccp1^{-/-}Ccp6^{-/-}* cortices showed organelle accumulations, axonal swellings, and cytoplasmic densification, while such figures were not observed in controls (representative examples are shown in Fig 3). In all observed cases, the myelin sheath appears rather well-preserved while the axon itself is heavily damaged. This suggests that degeneration of the axon is the primary defect, as opposed to the possibility that neurons degenerate following demyelination. Moreover, organelle accumulations in the degenerating axons are reminiscent of perturbations of axonal transport, which is a common defect in many neurodegenerative disorders (Millecamps & Julien, 2013; Brady & Morfini, 2017).

Excessive polyglutamylation affects cargo transport in neurons

To date, two potential molecular mechanisms that could perturb axonal transport in a polyglutamylation-dependent manner are known: either the microtubule tracks are damaged by excessive spastin-mediated severing—a process that is controlled by polyglutamylation (Lacroix *et al*, 2010; Valenstein & Roll-Mecak, 2016), or the transport itself is perturbed on the microtubule tracks.

Figure 2. Excessive polyglutamylation causes neurodegeneration of the cerebral cortex.

- Immunoblot analyses of tubulin polyglutamylation (antibody: polyE) in extracts of different brain regions of wild-type, *Ccp1^{-/-}*, *Ccp6^{-/-}*, and *Ccp1^{-/-}Ccp6^{-/-}* mice. In 3-week-old mice, hyperglutamylation is observed in cerebral cortex, cerebellum, and hippocampus of *Ccp1^{-/-}* and *Ccp1^{-/-}Ccp6^{-/-}* mice. In 2- and 5-month-old mice, hyperglutamylation is restricted to the cerebellum in *Ccp1^{-/-}* mice; however, it persists in all three brain regions of the *Ccp1^{-/-}Ccp6^{-/-}* mice (complete analysis in Fig EV1; α - and β -tubulin bands are indicated).
- Nissl-stained frontal sections of wild-type, *Ccp1^{-/-}*, *Ccp6^{-/-}*, and *Ccp1^{-/-}Ccp6^{-/-}* mice at 1 and 5 months, showing age-dependent thinning (arrowheads) of the cortex in *Ccp1^{-/-}Ccp6^{-/-}* mice (complete analysis in Appendix Fig S2A).
- Quantification of the thickness of motor and somatosensory cortex of 1- and 5-month-old mice shown in Appendix Fig S2. The single values shown in Appendix Fig S2B were averaged, and values from each genotype-specific group were tested against the average values of the remaining three genotypes (Appendix Fig S2C). Only the cortical thickness of 5-month-old *Ccp1^{-/-}Ccp6^{-/-}* mice is significantly decreased (mean \pm SEM; Mann–Whitney *t*-test).
- Immunohistochemistry of brain sections with anti-MAP2 antibody for visualization of neurons (layer V) and apical dendrites (layer IV) and with anti-GFAP antibody for reactive astrocytes (layer V). The complete analysis is shown in Figs EV2A and EV3A. Scale bars: 50 μ m.
- Quantifications of number of MAP2-positive neurons in layer V and of number of apical dendrites in layer IV (Fig EV2B) reveal reduced neuron number in layer V and reduced dendritic density in layer IV of 5-month-old *Ccp1^{-/-}Ccp6^{-/-}* mice. Quantification of the number of reactive astrocytes in layer V (Fig EV3B) shows a significant increase over wild-type in *Ccp1^{-/-}* and *Ccp6^{-/-}* mice; however, a much stronger increase is seen in *Ccp1^{-/-}Ccp6^{-/-}* mice. Complete analyses are shown in Figs EV2C and EV3C (mean \pm SEM; Student’s *t*-test).
- Immunohistochemistry of brain sections stained with SMI-32 antibody (a representative section of one brain per genotype group is shown, complete analysis in Appendix Fig S3). Neuronal SMI-32 labeling indicates increased axonal damage in the cortex of *Ccp1^{-/-}Ccp6^{-/-}* mice at 5 months. Scale bar: 100 μ m.
- Schematic representation of the experimental paradigm applied in this figure.

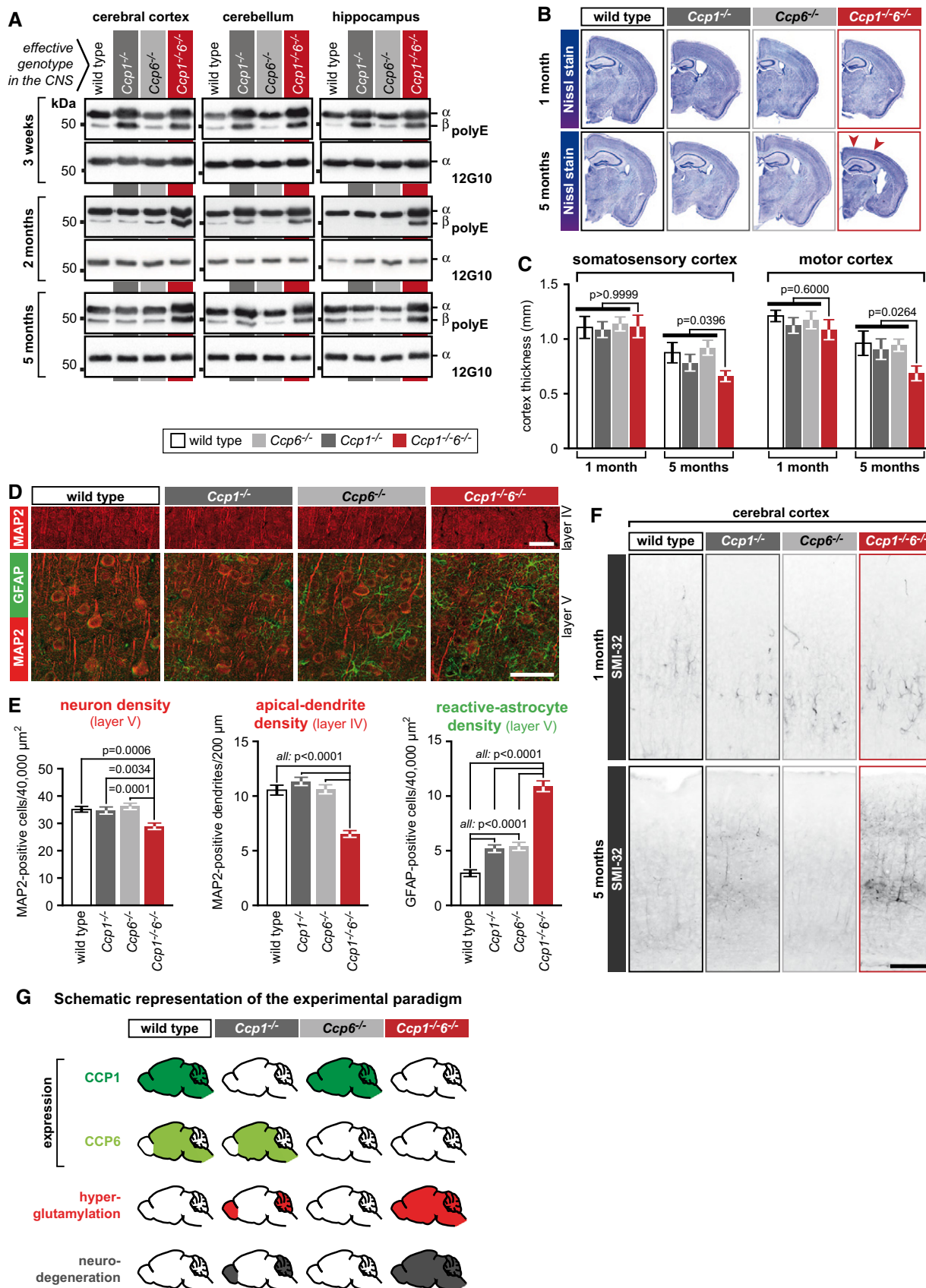


Figure 2.

We first tested whether excessive tubulin polyglutamylation could cause neurodegeneration by overactivating spastin-mediated severing in the affected neurons. Considering that removal of the polyglutamylase TLL1 had sustainably protected Purkinje cells from degenerating in our CCP1-deficient mouse model (Fig 1C and D), we argued that absence of spastin should have a similar effect in case spastin-mediated severing is causative for degeneration. We thus generated *Ccp1*^{-/-}*Spastin*^{-/-} mice and analyzed their cerebella at 1 month, when degeneration of Purkinje cells is almost completed in *Ccp1*^{-/-} (*pcd*) mice (Mullen et al, 1976). Strikingly, knockout of spastin did not slow down the degeneration

of Purkinje cells (Fig 4A and B, and Appendix Fig S4), suggesting that upregulated polyglutamylation levels did not significantly overactivate spastin-mediated microtubule severing in these cells. This can be explained by the particular mode of regulation of this process: While initial addition of polyglutamylation strongly activates microtubule severing by spastin (Lacroix et al, 2010), further accumulation of this modification leads to a plateau, and later even decreases the spastin activity (Valenstein & Roll-Mecak, 2016). It is thus possible that polyglutamylation levels of both wild-type and *Ccp1*^{-/-} neurons are within the plateau range of spastin activity.

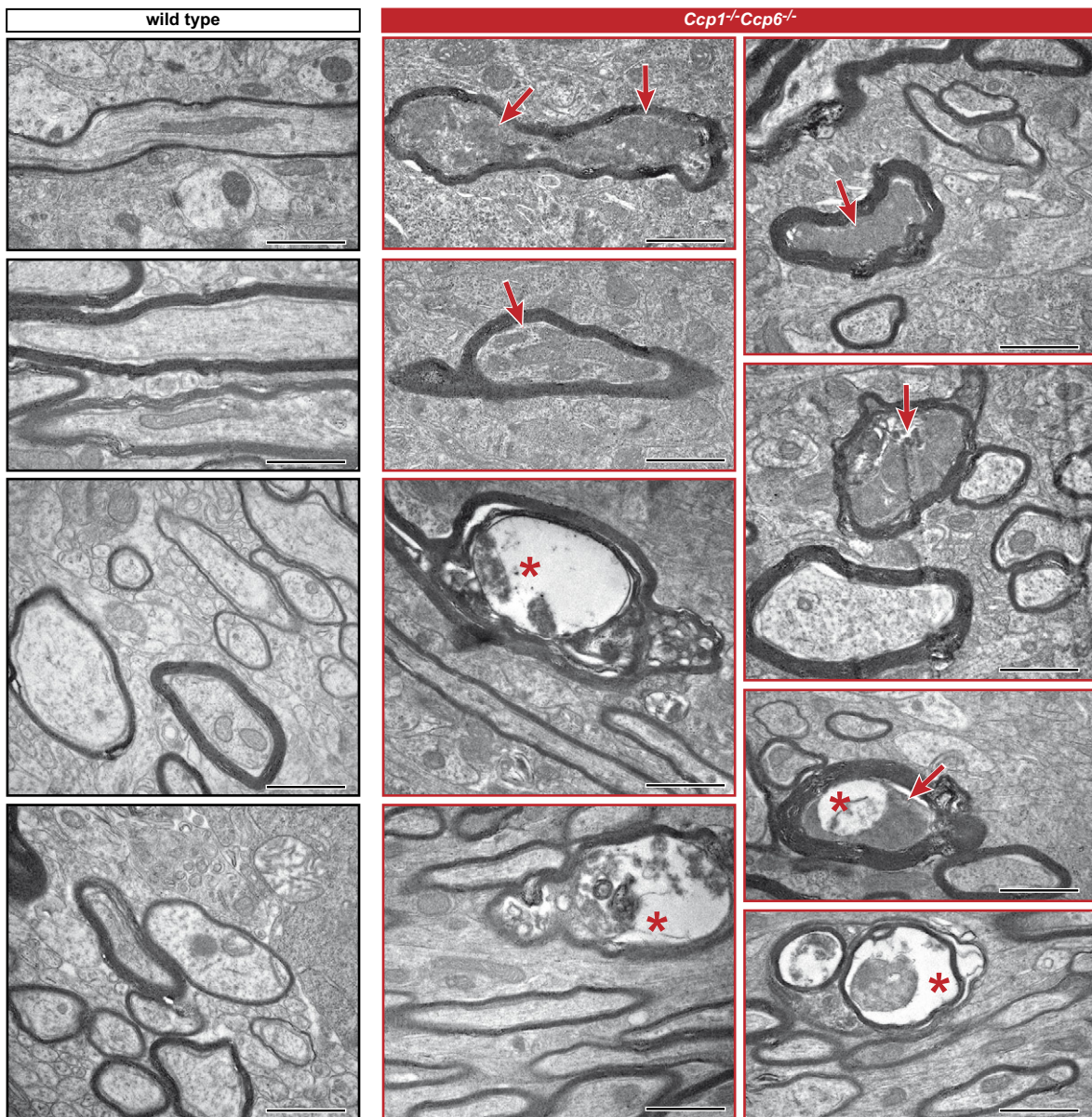


Figure 3. Ultrastructural analyses of axonal degeneration in the cerebral cortices of mice with hyperglutamylation.

Representative electron microscopy images of sections of wild-type and *Ccp1*^{-/-}*Ccp6*^{-/-} cerebral cortices with myelinated axons. In *Ccp1*^{-/-}*Ccp6*^{-/-} sections, several myelinated axons show signs of degeneration, such as accumulation of cellular organelles and cytoplasmic densification (arrows), or axonal lysis (stars). Note that only some axons in the observed sections displayed these phenotypes *Ccp1*^{-/-}*Ccp6*^{-/-}, while such figures were never observed in wild-type cortices. Scale bar: 1 μ m.

As these findings excluded a causative role of spastin-mediated microtubule severing in hyperglutamylation-induced degeneration of Purkinje cells, we next explored the impact of increased polyglutamylation on cargo trafficking in neurons. Our ultrastructural analyses of *Ccp1*^{-/-}*Ccp6*^{-/-} cortices had already indicated the presence of transport defects (Fig 3), and axon tracts of the few remaining Purkinje cells in *Ccp1*^{-/-} and *Ccp1*^{-/-}*Spastin*^{-/-} mice also displayed abnormal swellings (Fig 4C) reminiscent of perturbations in axonal transport (Balastik et al, 2008; Krstic & Knuesel, 2013).

To directly measure organelle transport in neurons with hyperglutamylation, we set up a cell-based assay. We chose primary

cultures of hippocampal neurons, as they contain mostly pyramidal neurons (Kaech & Banker, 2006), which are the ones that degenerate in the cortex of *Ccp1*^{-/-}*Ccp6*^{-/-} mice (Fig 2D and E). As our breeding schemes for mice have a low yield of the double-knockout genotype, we established an approach in which cultured *Ccp1*^{flox/flox}*Ccp6*^{flox/flox} neurons are transduced with a *cre*-recombinase-expressing lentivirus (Fig 5A). Expression of *cre*-recombinase results in efficient deletion of the two flox alleles (Appendix Fig S6D) and in a robust increase in tubulin polyglutamylation, while the levels of the modification remain unaffected in neurons transduced with control (GFP) virus (Fig 5B). This approach allowed us

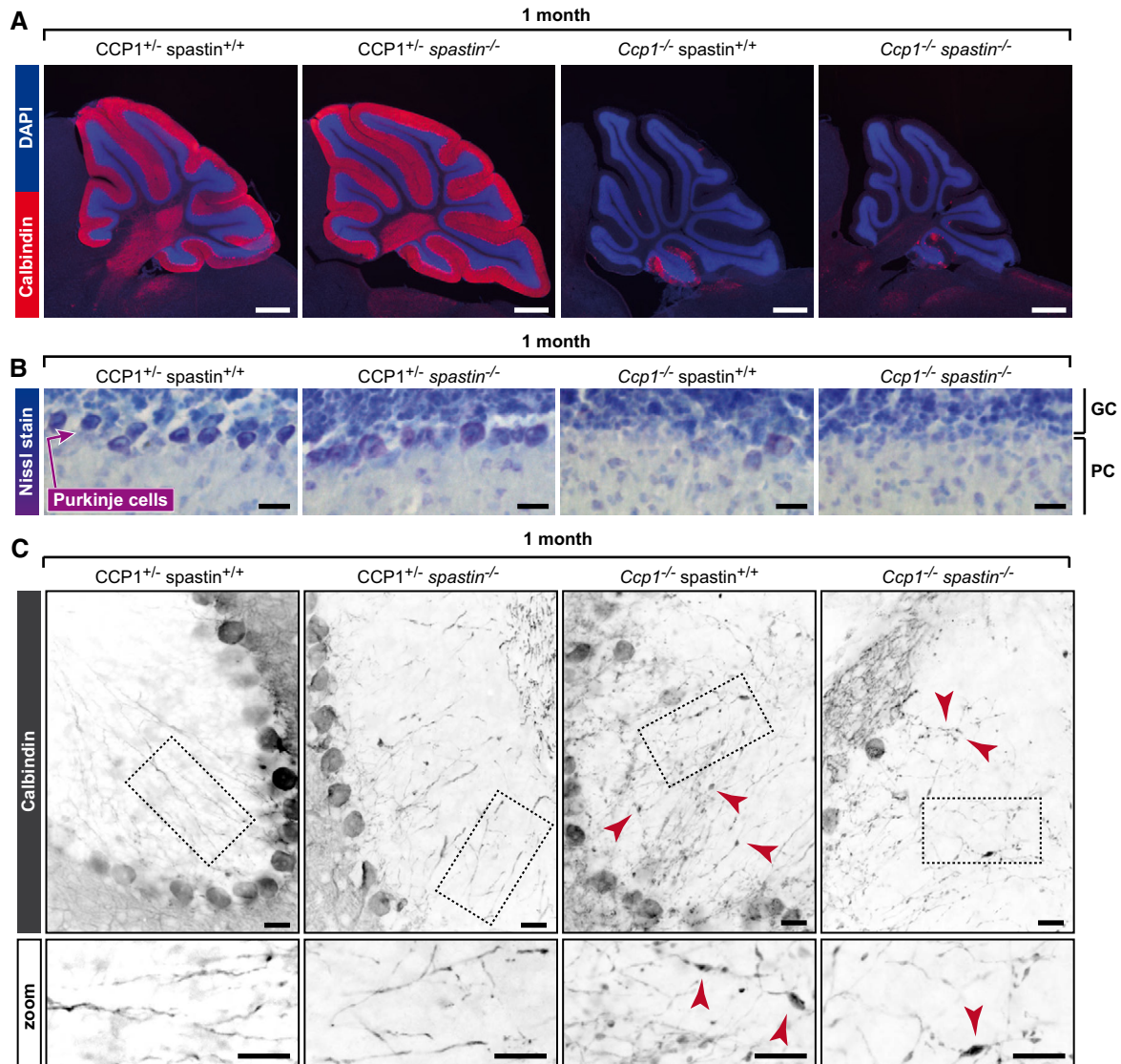


Figure 4. Spastin knockout does not protect Purkinje cells from degeneration in the pcd mouse.

A Fate of Purkinje cells in 1-month-old wild-type, *spastin*^{-/-}, *Ccp1*^{-/-}, and *Ccp1*^{-/-}*spastin*^{-/-} mice visualized with anti-calbindin antibody. *Ccp1*^{-/-} and *Ccp1*^{-/-}*spastin*^{-/-} mice show almost complete loss of the Purkinje cell layer. Scale bar: 500 μm.
 B Nissl staining shows the complete loss of Purkinje cells in *Ccp1*^{-/-} and *Ccp1*^{-/-}*spastin*^{-/-} mice. Scale bar: 20 μm. Purkinje cell layer (PC) and granule cell layer (GC) are indicated.
 C Calbindin staining of sections showing axons of Purkinje cells as in (A). While wild-type and *spastin*^{-/-} mice show normal axons, *Ccp1*^{-/-} and *Ccp1*^{-/-}*spastin*^{-/-} mice show axonal swellings (arrowheads) in the remaining Purkinje cells. Scale bars: 20 μm.

Figure 5. Axonal cargo transport is perturbed in neurons with excessive polyglutamylation.

- A Representation of the analysis scheme for axonal transport of mitochondria in $Ccp1^{flox/flox}Ccp6^{flox/flox}$ neurons. Hippocampal neurons from E17.5 embryos were cultured and transduced (on DIV0) with lentivirus expressing either GFP (control) or GFP-2A-cre (inducing conversion to $Ccp1^{-/-}Ccp6^{-/-}$). At DIV4, live neurons were stained with MitoTracker™ and mitochondria were imaged in GFP-positive cells for 1 min with a spinning disk microscope. Mitochondrial movements were plotted in kymographs for all the cells analyzed in each set and broken down into single runs without change in direction or speed. Anterograde and retrograde runs were color-coded in green and red, respectively, while immotile events are shown in blue.
- B Immunoblot of cell extracts from $Ccp1^{flox/flox}Ccp6^{flox/flox}$ hippocampal neurons without or after transduction with lentivirus expressing either GFP or GFP-2A-cre after 4 days in culture. Note the specific increase of polyglutamylation (polyE) in neurons transduced with GFP-2A-cre lentivirus.
- C–E All kymographs of one representative set of experiments. Mitochondrial movements (Movie EV1) were plotted in kymographs and analyzed as described in (A). Scale bars: 60 sec, 20 μ m. Analyses of (D) run length and (E) speed distribution, represented as scatter dot plots with each point representing a single run extracted from the kymographs shown in (C). Each group represents the pool of measurement of multiple neurons made in the experiment. The black line indicates the median of the distribution with whiskers at interquartile range. Numerical value of the medians is indicated below each plot.
- F, G Overall motility of mitochondria represented as fraction of time mitochondria spent in movement relative to the total number of mitochondria during the recording time of 60 s. Values (below plots) from one set of experiment (C) show a decrease of about 50% in $Ccp1^{-/-}Ccp6^{-/-}$ conditions, while (G) mitochondrial density is unaltered.
- H–K Statistical analyses of mitochondrial transport parameters of experiments shown in (D–G; Fig EV4A–D). Each bar represents the mean (\pm SEM) of medians of single experiments for run length (H) and speed (I) distributions, and average (\pm SEM) mitochondrial motility (J) and density (K) of all seven experimental sets. Values of fold change between control and $Ccp1^{-/-}Ccp6^{-/-}$ conditions are indicated below the graphs. Green bars are for anterograde, and red for retrograde transport events. Significance was tested using unpaired t-test. Average run length (H) as well as speed (I) showed no significant differences in these two parameters between control and $Ccp1^{-/-}Ccp6^{-/-}$ conditions. (J) The average of overall motility reveals an about 50% decrease in overall mitochondrial motility, while mitochondrial density (K) is unaltered between control and $Ccp1^{-/-}Ccp6^{-/-}$ conditions.

to directly compare neurons of the same cell culture with normal and excessive polyglutamylation. Finally, we decided to analyze mitochondria as they could be labeled without overexpression of marker proteins using the dye MitoTracker™.

Movement parameters of single mitochondria were analyzed following established approaches (Ghiretti *et al*, 2016) in neurons at 4 days in vitro (DIV4), as at this stage the neurons are fully polarized with a distinct axon (Kaech & Banker, 2006). In each experiment, mitochondrial movements in neurons transduced with either control or *cre*-expressing virus were recorded for 60 s in at least five different cells per condition. The longest neurites (axons) were manually traced (Fig 5A), and particle movements (Movie EV1) were converted to kymostacks and subsequently plotted as kymographs (Fig 5C shows all kymographs from one single experiment) using ImageJ (Schneider *et al*, 2012) with the KymoToolBox (Zala *et al*, 2013) plugin. Kymographs were further analyzed by tracing particle trajectories and dividing them into runs of uninterrupted movements at constant speed (Fig 5A and C). Measured parameters from each experimental condition (GFP versus GFP-2A-cre) were plotted to determine the distribution of movement parameters for all runs, from which we then derived the median for run length (Fig 5D) and speed (Fig 5E). The average median values of seven independent experiments (Figs 5D and E, and EV4A and B) revealed that increased polyglutamylation does neither affect the median run length (Fig 5H) nor run speed (Fig 5I) in neither anterograde nor retrograde direction.

By contrast, when we calculated the overall motility of mitochondria as the fraction of time mitochondria spent in movement relative to the total number of mitochondria during the recording time of 60 s (for more details, see Materials and methods), we found a strong reduction in both anterograde and retrograde directions in neurons transduced with GFP-2A-cre virus, i.e., in hyperglutamylation conditions for each single experiment (Figs 5F and EV4C). Statistical analyses of all seven individual experiments revealed a highly significant decrease of mitochondrial motility in neurons with excessive polyglutamylation in both transport directions (Fig 5J), while mitochondrial density was not affected (Figs 5G and K, and

EV4D). To verify that the observed effects are directly related to the knockout of *CCP1* and *CCP6* by cre-recombinase, we performed an equivalent set of experiments with primary neurons from wild-type mice. In wild-type neurons, expression of GFP-2A-cre did not affect any of the measured parameters (Fig EV5), which underpins the conclusion that the reduced motility in $Ccp1^{flox/flox}Ccp6^{flox/flox}$ neurons transduced with GFP-2A-cre virus is a specific result of the increased polyglutamylation.

Our data imply that excessive polyglutamylation in neurons negatively affects cargo traffic by reducing the overall movement of particles in these cells. How polyglutamylation regulates the transport of distinct axonal cargoes needs to be determined. The modification could either directly affect the efficiency of the molecular motors, such as kinesins and dynein (Ikegami *et al*, 2007; Sirajuddin *et al*, 2014), or alternatively affect the microtubule binding of other proteins that affect cargo transport (Kang *et al*, 2008; Barlan *et al*, 2013; Semenova *et al*, 2014; Monroy *et al*, 2018; Tymanskyj *et al*, 2018). Inefficient cargo transport could thus be one of the factors that lead to a progressive degeneration of neurons in the different mouse models we have described in this work.

Discussion

Research on the causes of human neurodegenerative diseases has identified several molecular mechanisms, such as protein misfolding and aggregation (Ross & Poirier, 2005), protein degradation deficiency (Huang & Figueiredo-Pereira, 2010), synaptic transmission of pathogenic proteins (Garden & La Spada, 2012), apoptosis and autophagy defects (Ghavami *et al*, 2014), or mitochondrial dysfunction and oxidative stress (Lin & Beal, 2006). Moreover, a growing body of evidence points toward dysfunctions of the microtubule cytoskeleton in the pathogenesis of neurodegenerative diseases (McMurray, 2000; Baird & Bennett, 2013; Chakraborti *et al*, 2016; Pellegrini *et al*, 2017); however, no unifying molecular mechanism affecting microtubule functions in these conditions has so far been found.

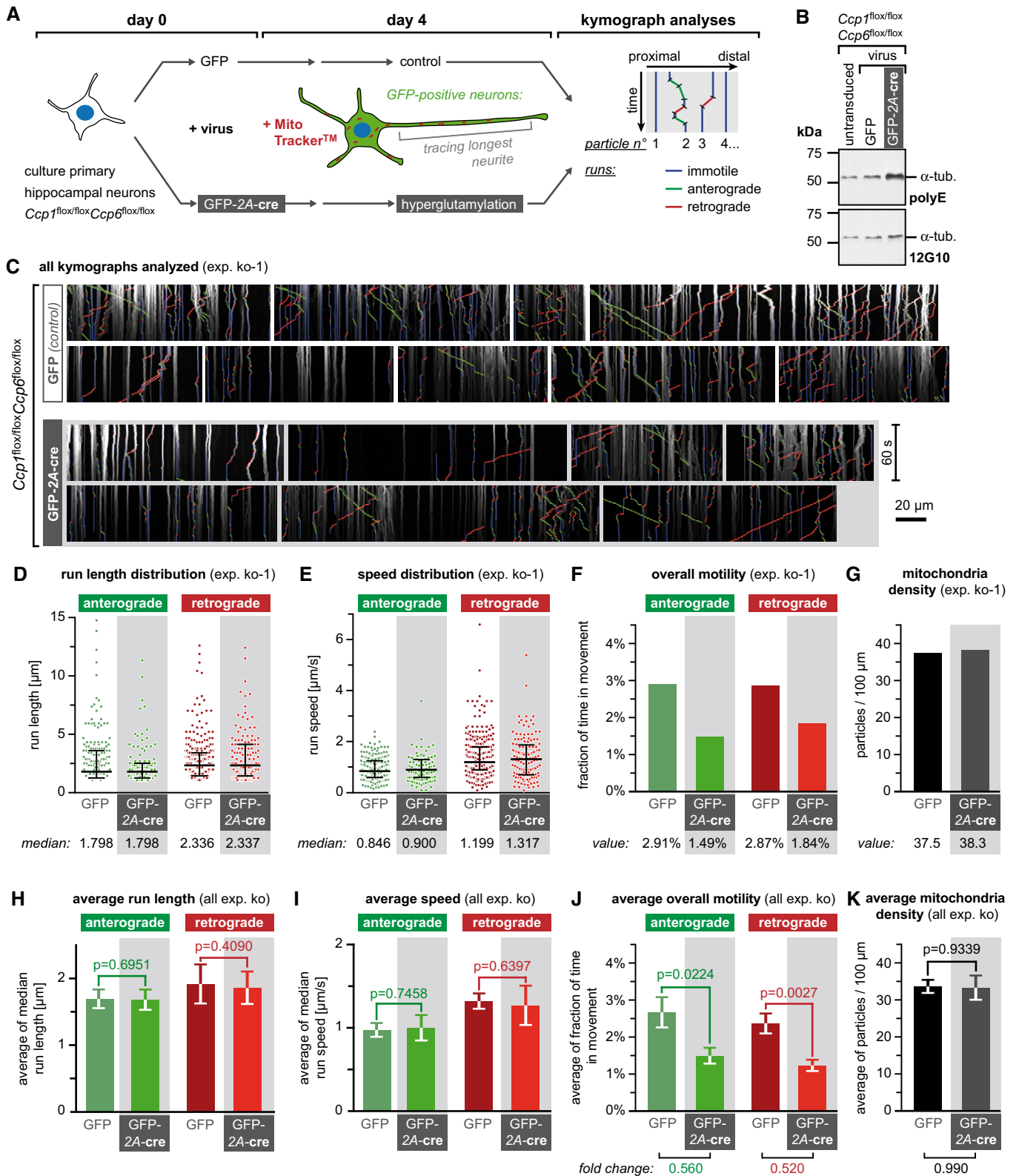


Figure 5.

Our study identifies polyglutamylation, a tubulin PTM that is particularly enriched on neuronal microtubules (Audebert *et al*, 1993, 1994; Redeker *et al*, 1998), as direct cause of the degeneration

of a variety of neurons in the central nervous system. By generating a panel of mouse models in which polyglutamylation levels are altered by the inactivation of enzymes involved in catalyzing

this PTM, we demonstrate that excess of polyglutamylation is sufficient to induce neurodegeneration in a cell-autonomous manner and that this mechanism is relevant in a variety of different neuron types. Moreover, we show that upregulation of polyglutamylation causes reduced efficiency of axonal transport, a common pathophysiological theme in age-related neurodegenerative disorders, such as Parkinson's, Huntington's and Alzheimer's diseases (Roy *et al*, 2005; De Vos *et al*, 2008; Barlan *et al*, 2013; Millecamps & Julien, 2013; Brady & Morfini, 2017). A recent model even suggests that transport defects and organelle accumulations, as we have also observed in our mouse models, could represent the upstream event of all pathogenic events in Alzheimer's disease (Small *et al*, 2017).

In an accompanying report (Shashi *et al*, 2018), we describe a first series of human patients carrying mutations in CCP1 (*AGTPBP1*) that lead to childhood-onset neurodegeneration. The disease progresses rapidly and mirrors the phenotypes of the *pcd* (*Ccp1*^{-/-}) mouse, which shows the relevance of disturbed polyglutamylation levels in human neurodegeneration and underpins the relevance of our mouse as model for neurodegenerative processes in humans. Considering the massive and rapid degeneration of neurons in *Ccp1*^{-/-} conditions, where polyglutamylation is measurably and rapidly accumulated, it is conceivable that more subtle alteration of this PTM could have the potential of being a so-far unrecognized risk factor for late-onset neurodegenerative disorders in humans. Such alterations may lead to an increased propensity for degeneration, which could be initiated either in conjunction with other factors or by accumulation of defects over longer periods of time. First indications for such links have recently emerged: For instance, subtle alterations of tubulin PTMs have been detected in brain tissue of Alzheimer's disease patients (Zhang *et al*, 2015; Vu *et al*, 2017), and another deglutamylase, CCP2 (encoded by the *AGBL2* gene), was linked to Alzheimer's disease by genome-wide association (Lambert *et al*, 2013) and proteome (Seyfried *et al*, 2017) studies. Although CCP2 is a deglutamylase with yet unknown functions, and knockout mice show no obvious defects in the nervous system (Tort *et al*, 2014), CCP2 dysfunction might lead to small alterations in polyglutamylation, resulting in accumulation of neuronal defects over the much longer lifespan of humans, and thus to late-onset neurodegeneration.

Our findings bolster the emerging importance of tubulin PTMs in neurological disorders. Tubulin acetylation for instance had previously been linked to neurodegenerative disorders such as Huntington's disease (Dompierre *et al*, 2007), Charcot-Marie-Tooth disease (d'Ydewalle *et al*, 2011; Kim *et al*, 2016), amyotrophic lateral sclerosis (ALS), and Parkinson's disease (Godena *et al*, 2014). Similar to polyglutamylation, changes in tubulin acetylation result in subtle alterations in microtubule functions, which could either be related to perturbed axonal transport or to altered mechanical properties of the microtubules (Xu *et al*, 2017), thus leading to a progressive degeneration of the affected neuron populations.

Finally, our observation that hyperglutamylation-induced neurodegeneration is entirely rescued by inactivation of the polyglutamylation enzyme TLL1 holds promise that specific inhibitors of this enzyme might bear a potential for therapeutic agents. Drugs specifically modulating levels of polyglutamylation and other tubulin PTMs might have the potential to treat disabling and often fatal neurodegeneration, for which, so far, no treatment is available.

Materials and Methods

Mouse lines and genotyping and breeding

Animal care and use for this study were performed in accordance with the recommendations of the European Community (2010/63/UE). Experimental procedures were specifically approved by the ethics committee of the Institut Curie CEEA-IC #118 (authorization no. 04395.03 given by National Authority) in compliance with the international guidelines.

Ccp1^{-/-} mice were described before (Munoz-Castaneda *et al*, 2018). *pcd* mice (BALB/cByJ-Agtppb1^{pcd-3J}/J; www.jax.org/strain/003237) were obtained from the Jackson Laboratory. *Ccp6*^{lox/lox} has been generated at the Mouse Clinical Institute (ICS, Illkirch, France) (see details in the Appendix). *Ttll1*^{tm1a(EUCOMM)Wtsi} mice were generated at EUCOMM ([http://www.mousephenotype.org/data/alleles/MGI:2443047/tm1a\(EUCOMM\)Wtsi](http://www.mousephenotype.org/data/alleles/MGI:2443047/tm1a(EUCOMM)Wtsi)). L7-cre mice were described before (Rico *et al*, 2004) and were a kind gift of B. Rico (King's College London, UK). *Spastin*^{-/-} mice were described before (Brill *et al*, 2016). Nestin-cre mice were described before (Tronche *et al*, 1999) and were a kind gift of F. Tronche (UPMC, CNRS, Paris, France).

For genotyping, DNA was extracted from ear or tail fragments, using proteinase K (#193504, MP Biomedicals). PCR-based genotyping was performed using primers and protocols listed in Appendix Fig S6A and B.

Mice of different genotypes were crossed to obtain animals of desired combinatorial genotypes. The schemes of crosses are shown in Appendix Fig S7. All cre-recombinase-expressing alleles were kept as heterozygotes and only bred to cre^{-/-} animals.

Sample preparation and immunoblotting

Mice were sacrificed, and brain and the spinal cord were rapidly dissected, crushed in 2.5× Laemmli buffer (5×: 450 mM DTT, 10% SDS, 400 mM Tris-HCl pH 6.8, 50% glycerol, bromophenol blue), and boiled for 5 min. Samples were further diluted, loaded on SDS-PAGE gels, and immunoblotted using antibodies listed in Appendix Table S1.

Transcardial perfusion

Animals were anesthetized using (Imalgène[®], 80–100 mg/ml)/Xylazine (Rompun[®], 5–10 mg/ml) and transcardially perfused first with PBS followed by 4% PFA (32% EM grade, #15714, EMS) in 0.1 M phosphate buffer (PB) pH 7.4. For electron microscopy, the fixative used was 2% PFA and 2% glutaraldehyde (25% EM grade, #16216, EMS) in 0.1 M PB pH 7.4. Organs were then dissected and postfixed in the 4% PFA in 0.1 M PB pH 7.4 overnight at 4°C, and then washed three times in 0.1 M PB pH 7.4.

Histology and immunohistochemistry

For frozen tissue sectioning, organs were cryoprotected in 30% sucrose, then embedded in Tissue-Tek[®] O.C.T. (#4483; Sakura Finetek), and frozen on dry ice. The tissue was then cut in 40-μm floating sections in the desired orientation (sagittal or frontal). Nissl staining was performed using 1% cresyl violet solution in 1% acetic

acid followed by destaining and dehydration. Immunostaining was performed using antibodies listed in Appendix Table S2. The sections were imaged using either the Leica DM6000B or the Nikon Ti-E spinning disk inverted confocal laser microscope, and the images were treated using the Adobe Photoshop or ImageJ (NIH) software (Schneider *et al*, 2012).

For paraffin sections, brains were embedded in paraffin using a tissue processor (Leica ASP200S), and 7- μ m-thick sagittal sections were cut with a microtome (Leica RM2255). For immunostaining, samples were treated as previously described (Balastik *et al*, 2015). Sections were imaged using the Nikon Eclipse Ti-U microscope. Cells and apical dendrites were counted using ImageJ cell counter plugin.

Electron microscopy

Perfusion-fixed brains were sliced into semi-thick sections with a vibratome, postfixed with 1.6% (v/v) paraformaldehyde and 2% (v/v) glutaraldehyde followed by a mix of 1% osmium tetroxide (v/v) in 100 mM cacodylate buffer. After dehydration, tissue slices were embedded in a mixture of pure ethanol and epoxy resin (Epon 812; Delta Microscopies, Toulouse, France). Areas of interest were oriented and re-embedded in blocks, and ultrathin sections (65 nm) were picked up on copper grids and then stained with UranylLess (Delta Microscopies, Toulouse, France) and lead citrate. Grids were examined with a Transmission Electron Microscope (H7650; Hitachi, Tokyo, Japan) at 80 kV.

Mouse hippocampal primary neuron culture, lentivirus production, and neuron transduction

Primary hippocampal neurons have been obtained as described before (Kaech & Banker, 2006).

Lentiviruses were produced as described before (Lahaye *et al*, 2016), using the pCMV-VSVG (a gift from B. Weinberg, Addgene plasmid #8454) plasmid for viral envelope components (Stewart *et al*, 2003) and psPAX2 (a gift from D. Trono, Addgene plasmid #12260) as packaging plasmid. GFP alone or GFP-2A-cre-recombinase (2A is a self-cleaving peptide allowing to generate GFP and cre-recombinase separately, from a single transcript (Kim *et al*, 2011)) was cloned into pTRIP (Gentili *et al*, 2015) vector under the CMV-enhanced chicken beta-actin (CAG) promoter (Alexopoulou *et al*, 2008).

Neurons were left untransduced or transduced with lentivirus encoding for GFP alone or GFP-2A-cre-recombinase. Cells were transduced at DIV0 (days in vitro).

Transport assays and quantification of mitochondrial motility

For all the transport experiments, neurons at DIV4 were incubated with 2 nM MitoTracker™ Red CMXRos for 1 min (#M7512; Thermo Fisher) and immediately imaged using a Nikon Ti-E spinning disk inverted confocal laser microscope. Mitochondrial movement was recorded at 37°C and 5% CO₂ in stream mode for 1 min. For every experiment, 4–9 neurons per treatment group were imaged.

Image processing was performed using ImageJ 1.47v (Schneider *et al*, 2012) extended with KymoToolBox (Zala *et al*, 2013).

Various transport parameters, including run length, run speed, and overall motility, were analyzed. Overall motility corresponds to the percentage of time particles spend in movement in the given

observation time: A motility of 100% would mean that all detected particles were in movement for the entire duration of the observation time.

Expanded View for this article is available online.

Acknowledgements

This work has received support under the program “Investissements d’Avenir” launched by the French Government and implemented by ANR with the references ANR-10-LBX-0038, ANR-10-IDEX-0001-02 PSL. The work of CJ was supported by the Institut Curie, the French National Research Agency (ANR) award ANR-12-BSV2-0007, the Institut National du Cancer (INCA) grants 2013-1-PL BIO-02-ICR-1 and 2014-PL BIO-11-ICR-1, and the Fondation pour la Recherche Medicale (FRM) grant DEQ20170336756. MMM is supported by the EMBO short-term fellowship ASTF 148-2015 and by the Fondation Vaincre Alzheimer grant FR-16055p, and JZ was supported by the Grant Agency of the Charles University, grant 682217. The work of MB was supported by Czech science foundation grant 16-15915S, the Marie Curie FP7-PEOPLE-2012-CIG grant 334431, and the European Regional Development Fund project, OPK Mikroskopický systém CZ.2.16/3.1.00/28034. The work of MK was supported by the German Research Foundation grant DFG-KN556/11-1. The mouse lines mutant for *CCP1*, *CCP6* and *TLL1* were established at the Mouse Clinical Institute (PHENOMIN-Institut Clinique de la Souris, MCI/ICS) in the Genetic Engineering and Model Validation Department by M.-C. Birling with funds from the CNRS. We thank C. Alberti, E. Belloir, F. Bertrand, V. Dangles-Marie, N. El-Tayara, S. Gadadhar, I. Grandjean, H. Hermange, N.-L. J. Nguyen, C. Serieysson, M. Sittewelle, A. Thadal, A. Volk (Institut Curie) for technical assistance, and R. Chabrier (Institut Curie) for graphical design. We are grateful to T. Harkany, G.G. Kovacs, and M.I. Lutz (Medical University Vienna, Austria) for help and advice with preliminary studies on the role of polyglutamylation in late-onset neurodegeneration, to B. Rico (King’s College London, UK) for providing us the L7-cre mouse line, and to the EUComm consortium for generating and providing the *Tll1*^{-/-} mouse. We are grateful to M.-N. Soler and C. Lovo from the PICT-IBiSA@Orsay Imaging Facility of the Institut Curie supported by the French National Research Agency through the “Investissement for the future” program (France-BioImaging, ANR-10-INSB-04), to C. Roulin from the RadExp facility for help with imaging, and to N. Manel (Institut Curie, Paris) for material and advice for the lentivirus production. We would like to thank M. Brill (Technical University Munich, Germany), C. González-Billault (University of Chile, Santiago, Chile), R. Martini (University Hospital Würzburg, Germany), J. Senderek (LMU Munich, Germany), and M. Sirajuddin (Instem, Bangalore, India) for instructive discussions.

Author contributions

Conceptualization: MMM, MB, CJ; Formal analysis: MMM, SB, JZ, SLa, AC, MB, CJ; Investigation: MMM, SB, JZ, SLa, PMS, SL; Resources: TJH, CB, AA, MK; Writing—original draft: MMM, CJ; Writing—review and editing: MMM, SB, MK, AC, MB, CJ; Supervision: MMM, AA, MK, ML, AC, MB, CJ; Project administration: MMM, CJ; Funding Acquisition: MMM, MB, CJ.

Conflict of interest

The authors declare that they have no conflict of interest.

References

- Aillaud C, Bosc C, Saoudi Y, Denarier E, Peris L, Sago L, Taulet N, Cieren A, Tort O, Magiera MM, Janke C, Redeker V, Andrieux A, Moutin M-J (2016)

- Evidence for new C-terminally truncated variants of alpha- and beta-tubulins. *Mol Biol Cell* 27: 640–653
- Alexopoulou AN, Couchman JR, Whiteford JR (2008) The CMV early enhancer/chicken beta actin (CAG) promoter can be used to drive transgene expression during the differentiation of murine embryonic stem cells into vascular progenitors. *BMC Cell Biol* 9: 2
- Audebert S, Desbruyeres E, Gruszczynski C, Koulakoff A, Gros F, Denoulet P, Eddé B (1993) Reversible polyglutamylation of alpha- and beta-tubulin and microtubule dynamics in mouse brain neurons. *Mol Biol Cell* 4: 615–626
- Audebert S, Koulakoff A, Berwald-Netter Y, Gros F, Denoulet P, Eddé B (1994) Developmental regulation of polyglutamylated alpha- and beta-tubulin in mouse brain neurons. *J Cell Sci* 107: 2313–2322
- Baird FJ, Bennett CL (2013) Microtubule defects & neurodegeneration. *J Genet Syndr Gene Ther* 4: 203
- Balastik M, Ferraguti F, Pires-da Silva A, Lee TH, Alvarez-Bolado G, Lu KP, Gruss P (2008) Deficiency in ubiquitin ligase TRIM2 causes accumulation of neurofilament light chain and neurodegeneration. *Proc Natl Acad Sci USA* 105: 12016–12021
- Balastik M, Zhou XZ, Alberich-Jorda M, Weissova R, Ziak J, Pazyra-Murphy MF, Cosker KE, Machonova O, Kozmikova I, Chen C-H, Pastorino L, Asara JM, Cole A, Sutherland C, Segal RA, Lu KP (2015) Prolyl isomerase pin1 regulates axon guidance by stabilizing CRMP2A selectively in distal axons. *Cell Rep* 13: 812–828
- Barlan K, Lu W, Gelfand VI (2013) The microtubule-binding protein ensconsin is an essential cofactor of kinesin-1. *Curr Biol* 23: 317–322
- Belvindrah R, Natarajan K, Shabajee P, Bruel-Jungerman E, Bernard J, Goutierre M, Moutkine I, Jaglin XH, Savariradjane M, Irinopoulou T, Ponce J-C, Janke C, Francis F (2017) Mutation of the alpha-tubulin Tuba1a leads to straighter microtubules and perturbs neuronal migration. *J Cell Biol* 216: 2443–2461
- Berezniuk I, Vu HT, Lyons PJ, Sironi JJ, Xiao H, Burd B, Setou M, Angeletti RH, Ikegami K, Fricker LD (2012) Cytosolic carboxypeptidase 1 is involved in processing alpha- and beta-tubulin. *J Biol Chem* 287: 6503–6517
- Bosch Grau M, Masson C, Gadadhar S, Rocha C, Tort O, Marques Sousa P, Vacher S, Bieche I, Janke C (2017) Alterations in the balance of tubulin glycylation and glutamylation in photoreceptors leads to retinal degeneration. *J Cell Sci* 130: 938–949
- Brady ST, Morfini GA (2017) Regulation of motor proteins, axonal transport deficits and adult-onset neurodegenerative diseases. *Neurobiol Dis* 105: 273–282
- Brettschneider J, Del Tredici K, Lee VM-Y, Trojanowski JQ (2015) Spreading of pathology in neurodegenerative diseases: a focus on human studies. *Nat Rev Neurosci* 16: 109–120
- Brill MS, Kleele T, Ruschkies L, Wang M, Marahori NA, Reuter MS, Hausrat TJ, Weigand E, Fisher M, Ahles A, Engelhardt S, Bishop DL, Kneussel M, Misgeld T (2016) Branch-specific microtubule destabilization mediates axon branch loss during neuromuscular synapse elimination. *Neuron* 92: 845–856
- Chakraborti S, Natarajan K, Curiel J, Janke C, Liu J (2016) The emerging role of the tubulin code: from the tubulin molecule to neuronal function and disease. *Cytoskeleton* 73: 521–550
- Craig AM, Banker G (1994) Neuronal polarity. *Annu Rev Neurosci* 17: 267–310
- De Vos KJ, Grierson AJ, Ackerley S, Miller CCJ (2008) Role of axonal transport in neurodegenerative diseases. *Annu Rev Neurosci* 31: 151–173
- Dent EW, Baas PW (2014) Microtubules in neurons as information carriers. *J Neurochem* 129: 235–239
- van Dijk J, Rogowski K, Miro J, Lacroix B, Eddé B, Janke C (2007) A targeted multienzyme mechanism for selective microtubule polyglutamylation. *Mol Cell* 26: 437–448
- Dompierre JP, Godin JD, Charrin BC, Cordelieres FP, King SJ, Humbert S, Saudou F (2007) Histone deacetylase 6 inhibition compensates for the transport deficit in Huntington's disease by increasing tubulin acetylation. *J Neurosci* 27: 3571–3583
- Eddé B, Rossier J, Le Caer JP, Desbruyeres E, Gros F, Denoulet P (1990) Posttranslational glutamylation of alpha-tubulin. *Science* 247: 83–85
- Fernandez-Gonzalez A, La Spada AR, Treadaway J, Higdon JC, Harris BS, Sidman RL, Morgan JI, Zuo J (2002) Purkinje cell degeneration (pcd) phenotypes caused by mutations in the axotomy-induced gene, *Nna1*. *Science* 295: 1904–1906
- Franker MAM, Hoogenraad CC (2013) Microtubule-based transport - basic mechanisms, traffic rules and role in neurological pathogenesis. *J Cell Sci* 126: 2319–2329
- Garden GA, La Spada AR (2012) Intercellular (mis)communication in neurodegenerative disease. *Neuron* 73: 886–901
- Geevasinga N, Menon P, Ozdinler PH, Kiernan MC, Vucic S (2016) Pathophysiological and diagnostic implications of cortical dysfunction in ALS. *Nat Rev Neurol* 12: 651–661
- Gentili M, Kowal J, Tkach M, Satoh T, Lahaye X, Conrad C, Boyron M, Lombard B, Durand S, Kroemer G, Loew D, Dalod M, Thery C, Manel N (2015) Transmission of innate immune signaling by packaging of cGAMP in viral particles. *Science* 349: 1232–1236
- Ghavami S, Shojaei S, Yeganeh B, Ande SR, Jangamreddy JR, Mehrpour M, Christoffersson J, Chaabane W, Moghadam AR, Kashani HH, Hashemi M, Owji AA, Los MJ (2014) Autophagy and apoptosis dysfunction in neurodegenerative disorders. *Prog Neurobiol* 112: 24–49
- Ghiretti AE, Thies E, Tokito MK, Lin T, Ostap EM, Kneussel M, Holzbaier ELF (2016) Activity-dependent regulation of distinct transport and cytoskeletal remodeling functions of the dendritic kinesin KIF21B. *Neuron* 92: 857–872
- Godena VK, Brookes-Hocking N, Moller A, Shaw G, Oswald M, Sancho RM, Miller CCJ, Whitworth AJ, De Vos KJ (2014) Increasing microtubule acetylation rescues axonal transport and locomotor deficits caused by LRRK2 Roc-COR domain mutations. *Nat Commun* 5: 5245
- Greer CA, Shepherd GM (1982) Mitral cell degeneration and sensory function in the neurological mutant mouse Purkinje cell degeneration (PCD). *Brain Res* 235: 156–161
- Hol EM, Pekny M (2015) Glial fibrillary acidic protein (GFAP) and the astrocyte intermediate filament system in diseases of the central nervous system. *Curr Opin Cell Biol* 32: 121–130
- Huang Q, Figueiredo-Pereira ME (2010) Ubiquitin/proteasome pathway impairment in neurodegeneration: therapeutic implications. *Apoptosis* 15: 1292–1311
- Ikegami K, Heier RL, Taruishi M, Takagi H, Mukai M, Shimma S, Taira S, Hatanaka K, Morone N, Yao I, Campbell PK, Yuasa S, Janke C, Macgregor GR, Setou M (2007) Loss of alpha-tubulin polyglutamylation in ROSA22 mice is associated with abnormal targeting of KIF1A and modulated synaptic function. *Proc Natl Acad Sci USA* 104: 3213–3218
- Janke C, Rogowski K, Wloga D, Regnard C, Kajava AV, Strub J-M, Temurak N, van Dijk J, Boucher D, van Dorsselaer A, Suryavanshi S, Gaertig J, Eddé B (2005) Tubulin polyglutamylase enzymes are members of the TTL domain protein family. *Science* 308: 1758–1762
- Janke C, Bulinski JC (2011) Post-translational regulation of the microtubule cytoskeleton: mechanisms and functions. *Nat Rev Mol Cell Biol* 12: 773–786
- Janke C (2014) The tubulin code: molecular components, readout mechanisms, and functions. *J Cell Biol* 206: 461–472
- Kaech S, Banker G (2006) Culturing hippocampal neurons. *Nat Protoc* 1: 2406–2415

- Kalinina E, Biswas R, Berezniuk I, Hermoso A, Aviles FX, Fricker LD (2007) A novel subfamily of mouse cytosolic carboxypeptidases. *FASEB J* 21: 836–850
- Kang J-S, Tian J-H, Pan P-Y, Zald P, Li C, Deng C, Sheng Z-H (2008) Docking of axonal mitochondria by syntaphilin controls their mobility and affects short-term facilitation. *Cell* 132: 137–148
- Kim JY, Shen S, Dietz K, He Y, Howell O, Reynolds R, Casaccia P (2010) HDAC1 nuclear export induced by pathological conditions is essential for the onset of axonal damage. *Nat Neurosci* 13: 180–189
- Kim JH, Lee S-R, Li L-H, Park H-J, Park J-H, Lee KY, Kim M-K, Shin BA, Choi S-Y (2011) High cleavage efficiency of a 2A peptide derived from porcine teschovirus-1 in human cell lines, zebrafish and mice. *PLoS ONE* 6: e18556
- Kim J-Y, Woo S-Y, Hong YB, Choi H, Kim J, Choi H, Mook-Jung I, Ha N, Kyung J, Koo SK, Jung S-C, Choi B-O (2016) HDAC6 inhibitors rescued the defective axonal mitochondrial movement in motor neurons derived from the induced pluripotent stem cells of peripheral neuropathy patients with HSPB1 mutation. *Stem Cells Int* 2016: 9475981
- Krstic D, Knuesel I (2013) Deciphering the mechanism underlying late-onset Alzheimer disease. *Nat Rev Neurol* 9: 25–34
- Lacroix B, van Dijk J, Gold ND, Guizetti J, Aldrian-Herrada G, Rogowski K, Gerlich DW, Janke C (2010) Tubulin polyglutamylation stimulates spastin-mediated microtubule severing. *J Cell Biol* 189: 945–954
- Lahaye X, Satoh T, Gentili M, Cerboni S, Silvin A, Conrad C, Ahmed-Belkacem A, Rodriguez EC, Guichou J-F, Bosquet N, Piel M, Le GR, King MC, Pawlowsky J-M, Manel N (2016) Nuclear envelope protein SUN2 promotes cyclophilin-A-dependent steps of HIV replication. *Cell Rep* 15: 879–892
- Lambert JC, Ibrahim-Verbaas CA, Harold D, Naj AC, Sims R, Bellenguez C, DeStafano AL, Bis JC, Beecham GW, Grenier-Boley B, Russo G, Thornton-Wells TA, Jones N, Smith AV, Chouraki V, Thomas C, Ikram MA, Zelenika D, Vardarajan BN, Kamatani Y et al (2013) Meta-analysis of 74,046 individuals identifies 11 new susceptibility loci for Alzheimer's disease. *Nat Genet* 45: 1452–1458
- LaVail MM, Blanks JC, Mullen RJ (1982) Retinal degeneration in the pcd cerebellar mutant mouse. I. Light microscopic and autoradiographic analysis. *J Comp Neurol* 212: 217–230
- Lin MT, Beal MF (2006) Mitochondrial dysfunction and oxidative stress in neurodegenerative diseases. *Nature* 443: 787–795
- Liu G, Dwyer T (2014) Microtubule dynamics in axon guidance. *Neurosci Bull* 30: 569–583
- McMurray CT (2000) Neurodegeneration: diseases of the cytoskeleton? *Cell Death Differ* 7: 861–865
- Millecamps S, Julien J-P (2013) Axonal transport deficits and neurodegenerative diseases. *Nat Rev Neurosci* 14: 161–176
- Monroy BY, Sawyer DL, Ackermann BE, Borden MM, Tan TC, Ori-McKenney KM (2018) Competition between microtubule-associated proteins directs motor transport. *Nat Commun* 9: 1487
- Mullen RJ, Eicher EM, Sidman RL (1976) Purkinje cell degeneration, a new neurological mutation in the mouse. *Proc Natl Acad Sci USA* 73: 208–212
- Munoz-Castaneda R, Diaz D, Peris L, Andrieux A, Bosc C, Munoz-Castaneda JM, Janke C, Alonso JR, Moutin M-J, Weruaga E (2018) Cytoskeleton stability is essential for the integrity of the cerebellum and its motor- and affective-related behaviors. *Sci Rep* 8: 3072
- O'Gorman S, Sidman RL (1985) Degeneration of thalamic neurons in "Purkinje cell degeneration" mutant mice. I. Distribution of neuron loss. *J Comp Neurol* 234: 277–297
- Pellegrini L, Wetzell A, Granno S, Heaton G, Harvey K (2017) Back to the tubule: microtubule dynamics in Parkinson's disease. *Cell Mol Life Sci* 74: 409–434
- Redeker V, Rossier J, Frankfurter A (1998) Posttranslational modifications of the C-terminus of alpha-tubulin in adult rat brain: alpha 4 is glutamylated at two residues. *Biochemistry* 37: 14838–14844
- Rico B, Beggs HE, Schahin-Reed D, Kimes N, Schmidt A, Reichardt LF (2004) Control of axonal branching and synapse formation by focal adhesion kinase. *Nat Neurosci* 7: 1059–1069
- Rodriguez de la Vega M, Sevilla RG, Hermoso A, Lorenzo J, Tanco S, Diez A, Fricker LD, Bautista JM, Aviles FX (2007) Nna1-like proteins are active metallo-carboxypeptidases of a new and diverse M14 subfamily. *FASEB J* 21: 851–865
- Rogowski K, van Dijk J, Magiera MM, Bosc C, Deloulme J-C, Bosson A, Peris L, Gold ND, Lacroix B, Bosch Grau M, Bec N, Larroque C, Desagher S, Holzer M, Andrieux A, Moutin M-J, Janke C (2010) A family of protein-deglutamylating enzymes associated with neurodegeneration. *Cell* 143: 564–578
- Ross CA, Poirier MA (2005) Opinion: what is the role of protein aggregation in neurodegeneration? *Nat Rev Mol Cell Biol* 6: 891–898
- Roy S, Zhang B, Lee VM-Y, Trojanowski JQ (2005) Axonal transport defects: a common theme in neurodegenerative diseases. *Acta Neuropathol* 109: 5–13
- Schneider CA, Rasband WS, Eliceiri KW (2012) NIH image to ImageJ: 25 years of image analysis. *Nat Methods* 9: 671–675
- Semenova I, Ikeda K, Resaul K, Kraikivski P, Aguiar M, Gygi S, Zaliapin I, Cowan A, Rodionov V (2014) Regulation of microtubule-based transport by MAP4. *Mol Biol Cell* 25: 3119–3132
- Seyfried NT, Dammer EB, Swarup V, Nandakumar D, Duong DM, Yin L, Deng Q, Nguyen T, Hales CM, Wingo T, Glass J, Gearing M, Thambisetty M, Troncoso JC, Geschwind DH, Lah JJ, Levey AI (2017) A multi-network approach identifies protein-specific co-expression in asymptomatic and symptomatic Alzheimer's disease. *Cell Syst* 4: 60–72 e64
- Shashi V, Magiera MM, Klein D, Zaki M, Schoch K, Rudnik-Schöneborn S, Norman A, Lopes Abath Neto O, Dusl M, Yuan X, Bartesaghi L, De Marco P, Alfares AA, Marom R, Arold ST, Guzmán-Vega FJ, Pena LDM, Smith EC, Steinlin M, Babiker MOE et al (2018) Loss of tubulin deglutamylase CCP1 causes infantile-onset neurodegeneration. *EMBO J* 37: e100540
- Shimada A, Tsuzuki M, Keino H, Satoh M, Chiba Y, Saitoh Y, Hosokawa M (2006) Apical vulnerability to dendritic retraction in prefrontal neurones of ageing SAMP10 mouse: a model of cerebral degeneration. *Neuropathol Appl Neurobiol* 32: 1–14
- Sirajuddin M, Rice LM, Vale RD (2014) Regulation of microtubule motors by tubulin isoforms and post-translational modifications. *Nat Cell Biol* 16: 335–344
- Small SA, Simoes-Spassov S, Mayeux R, Petsko GA (2017) Endosomal traffic jams represent a pathogenic hub and therapeutic target in Alzheimer's disease. *Trends Neurosci* 40: 592–602
- Stewart SA, Dykxhoorn DM, Palliser D, Mizuno H, Yu EY, An DS, Sabatini DM, Chen ISY, Hahn WC, Sharp PA, Weinberg RA, Novina CD (2003) Lentivirus-delivered stable gene silencing by RNAi in primary cells. *RNA* 9: 493–501
- Tanco S, Tort O, Demol H, Aviles FX, Gevaert K, Van Damme P, Lorenzo J (2015) C-terminomics screen for natural substrates of cytosolic carboxypeptidase 1 reveals processing of acidic protein C termini. *Mol Cell Proteomics* 14: 177–190
- Tort O, Tanco S, Rocha C, Bieche I, Seixas C, Bosc C, Andrieux A, Moutin M-J, Xavier Aviles F, Lorenzo J, Janke C (2014) The cytosolic carboxypeptidases CCP2 and CCP3 catalyze posttranslational removal of acidic amino acids. *Mol Biol Cell* 25: 3017–3027
- Tronche F, Kellendonk C, Kretz O, Gass P, Anlag K, Orban PC, Bock R, Klein R, Schutz G (1999) Disruption of the glucocorticoid receptor gene in the nervous system results in reduced anxiety. *Nat Genet* 23: 99–103

- Tymanskyj SR, Yang BH, Verhey KJ, Ma L (2018) MAP7 regulates axon morphogenesis by recruiting kinesin-1 to microtubules and modulating organelle transport. *Elife* 7: e36374
- Valenstein ML, Roll-Mecak A (2016) Graded control of microtubule severing by tubulin glutamylation. *Cell* 164: 911–921
- Vu HT, Akatsu H, Hashizume Y, Setou M, Ikegami K (2017) Increase in alpha-tubulin modifications in the neuronal processes of hippocampal neurons in both kainic acid-induced epileptic seizure and Alzheimer's disease. *Sci Rep* 7: 40205
- Wang Y, Mandelkow E (2016) Tau in physiology and pathology. *Nat Rev Neurosci* 17: 22–35
- Watson DF, Fittro KP, Hoffman PN, Griffin JW (1991) Phosphorylation-related immunoreactivity and the rate of transport of neurofilaments in chronic 2,5-hexanedione intoxication. *Brain Res* 539: 103–109
- Xu Z, Schaedel L, Portran D, Aguilar A, Gaillard J, Marinkovich MP, Thery M, Nachury MV (2017) Microtubules acquire resistance from mechanical breakage through intraluminal acetylation. *Science* 356: 328–332
- d'Ydewalle C, Krishnan J, Chiheb DM, Van Damme P, Irobi J, Kozikowski AP, Vanden Berghe P, Timmerman V, Robberecht W, Van Den Bosch L (2011) HDAC6 inhibitors reverse axonal loss in a mouse model of mutant HSPB1-induced Charcot-Marie-Tooth disease. *Nat Med* 17: 968–974
- Zala D, Hinkelmann M-V, Yu H, Lyra da Cunha MM, Liot G, Cordelieres FP, Marco S, Saudou F (2013) Vesicular glycolysis provides on-board energy for fast axonal transport. *Cell* 152: 479–491
- Zhang F, Su B, Wang C, Siedlak SL, Mondragon-Rodriguez S, Lee H-G, Wang X, Perry G, Zhu X (2015) Posttranslational modifications of alpha-tubulin in alzheimer disease. *Transl Neurodegener* 4: 9